Chem Soc Rev

Prospects for Point of Care Pathogen Diagnostics of Surface-enhanced Raman Scattering (SERS)

Journal:	*Chemical Society Reviews*
Manuscript ID	CS-REV-11-2015-000828.R2
Article Type:	Review Article
Date Submitted by the Author:	24-Mar-2016
Complete List of Authors:	Granger, Jennifer; University of Utah, Nano Institute of Utah Schlotter, Nicholas; University of Utah, Nano Institute of Utah Crawford, Alexis; University of Utah, Chemistry Porter, Marc; University of Utah, Chemistry

Prospects for Point of Care Pathogen Diagnostics Using Surface-enhanced Raman Scattering (SERS)

Jennifer H. Granger,[1] Nicholas E. Schlotter,[1,2] Alexis C. Crawford,[3] and Marc D. Porter[1,3,4]
[1]Nano Institute of Utah, [3]Department of Chemistry, and [4]Department of Chemical Engineering, University of Utah, Salt Lake City, UT 84112, USA
[2]Department of Chemistry, Hamline University, Saint Paul, MN 55104, USA

Abstract: Surface-enhanced Raman scattering (SERS) has enabled the detection of pathogens and disease markers at extremely low levels. This review examines the potential impact of SERS in addressing unmet needs in pathogen diagnostics both in a traditional clinical setting and in the point of care (POC) arena. It begins by describing the strengths and weaknesses of today's diagnostics technologies in order to set a contextual stage for an overview which highlights a few of the many recent developments using SERS in biodefense, human and animal health, and monitoring food and water safety. These sections are followed by discussions of the challenges for the translation of these developments to POC settings, including the performance attributes and metrics for quantification of analytical and clinical figures of merit (*e.g.*, limit of detection and clinical accuracy), and the pathways for large-scale test validation and the build-out of instrumentation and tests kits for POC deployment.

Introduction

The past several years have witnessed a number of remarkable advances in the capabilities of diagnostic tests for human and animal health, food and water safety, and homeland security.[1] Scientists are now armed with techniques to detect markers of infectious disease, cancer, and other disorders at exceedingly low levels in serum, urine, and other complex sample matrices. This capability stems largely from methods based on extrinsic and intrinsic amplification. As shown in **Figure 1**, there are two extrinsic amplification (EA) strategies: target amplification (TA) and signal amplification (SA). TA replicates the target, which is usually DNA. In this approach, a selective binding event initiates the catalytic production of huge numbers of target. The polymerase chain reaction (PCR), depicted in **Figure 1A**, is the best known TA technique.[2] PCR can produce billions of target copies, enabling the measurement of only a few copies of the original nucleic acid sequence.

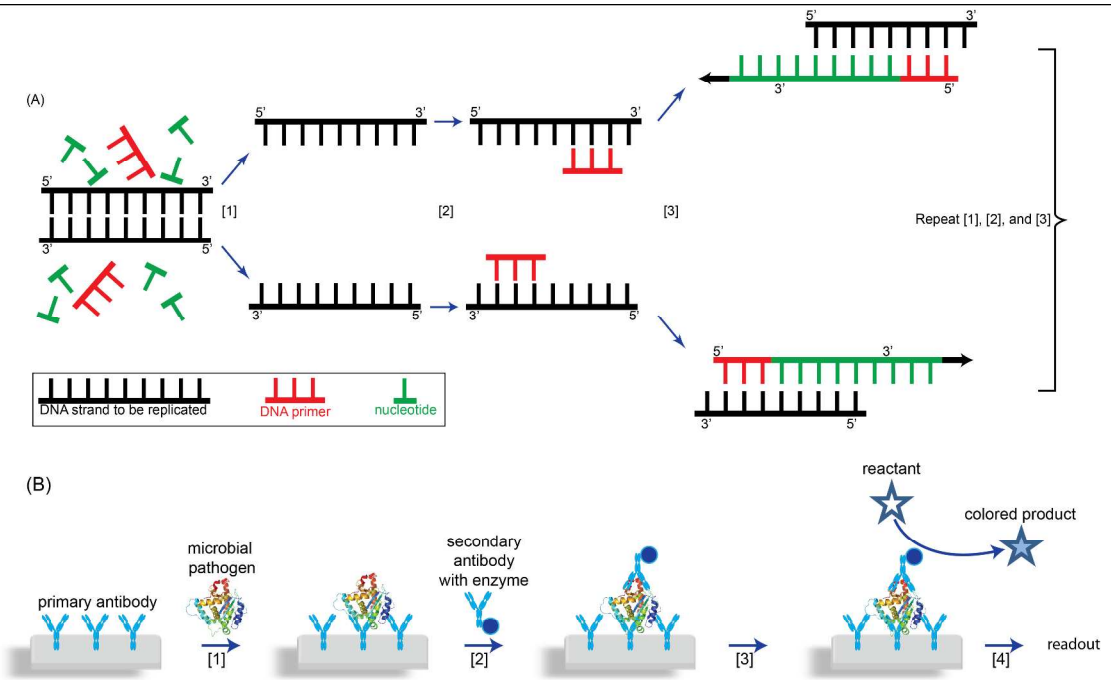

Figure 1. (A) PCR: [1] thermal denaturation; [2] primer annealing; [3] elongation growth of complement; and repeat 1, 2, and 3 as needed for detection (typically 20 to 40 times). (B) ELISA: [1] target capture; [2] target labeling; [3] enzymatic generation of chromophore; and [4] optical readout.

SA takes a different tactic. In this case, a recognition event conjugates a target to a catalytic species that then generates a molecular product (different from the target) in large numbers for indirect detection. The most established SA technique is the enzyme-linked immunosorbent assay (ELISA),[3] overviewed in **Figure1B**. In ELISA, a target is selectively captured by a surface-bound antibody and then "sandwiched" by being tagged with a second antibody that has been coupled to an enzyme. Upon addition of a substrate, an enzymatic reaction generates large numbers of a chromogenic product. ELISA can detect targets at picomolar (pM) levels. The recent development of "digital ELISA" has pushed detection down by another factor of 100-1000,[4] even lower marker levels (~4×10^{-20} M for prostate-specific antigen)[5] were detected when using the enzyme label to grow gold nanoparticles (AuNPs).

Conversely, intrinsic amplification (IA) does not rely on catalytic replication for a large signal enhancement but rather on a number of physical phenomena. This approach is exemplified by the design of colorimetric spectrometric methods. According to the Beer-Lambert Law, the limit of detection (*LoD*) is directly proportional to the molar absorptivity (ε) of the complex formed by the target and ligand. The synthesis of ligands that selectively bind to a target and form a colorimetric complex with a large ε is therefore a strategy common to many optical measurements for enhanced detection. IA mechanisms are found in other spectroscopies, including that from optical resonance which gives rise to the amplified signal strength in resonance Raman scattering.

In keeping with the focus of this review, there are a number of approaches to IA that take advantage of the properties of nanometer-sized materials. One example alters the labeling strategy used in ELISA by tagging the captured target on the surface of a

quartz crystal microbalance (QCM) with antibody-modified AuNPs and measuring the change in the gravimetrically-based resonance frequency (Δf_g).[6] Per Sauerbrey's equation, Δf_g is directly proportional to the change in QCM mass loading (ΔM). As a result, the much higher density of the AuNP label over that of an antibody alone improves the *LoD*. Other approaches to signal enhancement with a nanomaterials origin can be found in the fields of spintronics[7] and plasmonics.[8] Spintronics utilizes the spin-dependent conductivity of electrons in magnetic materials. This phenomenon serves as the basis of the giant magnetoresistance effect used in today's hard disk drives and has been recently incorporated as a transduction scheme in diagnostic tests.[9, 10]

As opposed to the spin-dependent process of spintronics, plasmonics involves phenomena due to the collective oscillation of free surface electrons in a metal due to resonance excitation by electromagnetic radiation.[11, 12] While surface plasmon resonance (SPR) can propagate an electromagnetic wave along a metal/dielectric interface,[11, 13, 14] it is the localized surface plasmon resonance (LSPR) that is central to this review.[15-18] LSPR creates an amplified electric field near nanometer-sized features (*e.g.*, nanoparticles and asperities of roughened metal surfaces) of metals like silver and gold, which, owing to resonances in the visible and near infrared spectral region, are the most commonly used nanomaterials in diagnostic test development.

LSPR is the principle underpinning of surface-enhanced Raman scattering (SERS).[19-22] Raman scattering, like infrared spectroscopy, probes molecular vibrations, but is an inherently much weaker process. While the origin of SERS continues to be studied in ever increasing detail,[23, 24] the amplification of the electric field that occurs in the LSPR-based "zone of enhancement,"[25-27] which undergoes an extremely sharp

decay (~10^{-10}) with increased distance from the surface,[28, 29] can enable single molecule detection.[30] Since its discovery in the late 1970's,[31-33] SERS has been applied to a wide range of measurements in analytical and biological chemistry.[23, 34-48] Vo-Ding and co-workers were the first to report on the potential of SERS as a spectrochemical methodology in 1984.[49] Not long thereafter, Cotton and colleagues described an approach to apply SERS to immunoassays.[34] Indeed, SERS-based immunoassays have become widespread,[23, 34-37, 39, 42, 44, 45, 47, 48] and this review is structured to discuss its use for pathogen detection and its potential in point-of-need (POC) applications. This review therefore: (1) examines the strengths and weaknesses of today's diagnostic tests for pathogens; (2) highlights a few of the many exciting developments demonstrating the potential of SERS in pathogen detection; and (3) discusses obstacles faced when attempting to move SERS-based diagnostic tests from the laboratory to field applications. Due to the breadth of this area, readers are referred to recent reviews,[50, 51] which provide a much broader and more in-depth discussion of SERS as an emerging addition to the diagnostics toolbox. With respect to the transition to the clinical and POC settings, we will draw both on recent reports on the obstacles faced when making such a move and on our own ongoing experiences. The review closes with a brief projection of when the promise of SERS diagnostics will be realized.

Merits of SERS in Pathogen Detection

Events like the recent Ebola pandemic and the Anthrax attacks that occurred after the destruction of the Twin Towers on September 11, 2001, have pushed the development of tests for the rapid, reliable detection of pathogens at the highest

possible priority.[52] Nonetheless, shortfalls in today's pathogen detection/surveillance capabilities compromise responses to public health emergencies.[53] The overall challenge reflects limitations in the speed, sensitivity, ease-of-use, and cost of existing diagnostic methods (*e.g.,* culture[54-56] and ELISA[57]), all of which are imperatives when developing a POC test. Indeed, important advances to meeting these needs are on the horizon, including those based on PCR,[58] SPR,[59] dynamic light scattering (DLS),[60] fluorescence,[61-63] magnetic separations,[64] chemiluminescence,[65] and SERS.[66]

The use of SERS for detection in diagnostics is founded on several attributes. First, the widths of Raman spectral features are 10-100 times narrower than those of fluorescence; this minimizes spectral overlap between different labels that are used in SERS methods for indirect quantification, making more extensive multiplexing possible. Second, the optimum excitation wavelength for SERS is linked to nanoparticle size, shape, composition and dielectric environment; as described in portions of the following sections, only one laser excitation wavelength is required for multiplexing.

These strengths of SERS have been exploited by our group[39, 67, 68] and others[34, 69, 70] by using an immunosorbent assay format like that in **Figure 2**. This approach has

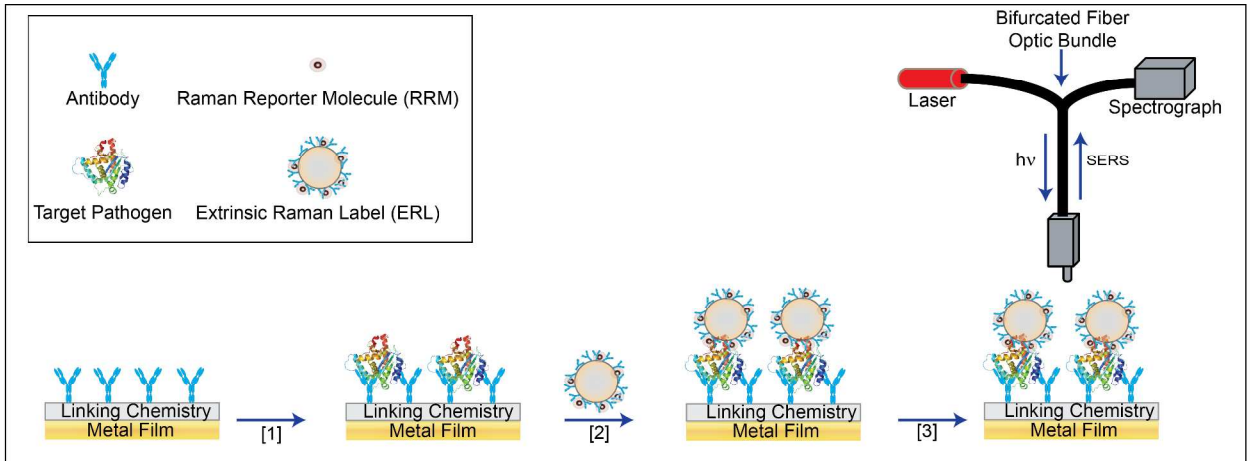

Figure 2. Illustration of a SERS Immunoassay. [1] Capture of target by modified surface, [2] Labeling with modified nanoparticles, and [3] Readout with Raman spectrometer.

many similarities to ELISA and other types of assay platforms. The difference in construction between SERS and other types of assay platforms rests in the capture address, which is usually an antibody (Ab) coated on a metal film (*e.g.,* gold), and the label, which consist of gold or silver nanoparticles typically coated with a Raman-active reporter molecule (RRM) and an antigen-specific layer of Abs. These modified nanoparticles are referred to as extrinsic Raman labels (ERLs). Importantly, ERLs are designed to: (1) fully exploit the strong SERS signal from RRMs immobilized on AuNPs; (2) selectively tag the captured target; and (3) facilitate multiplexed detection with a single excitation wavelength when using different RRMs. Given the noted sharp decay of the amplified electric field as the distance from the AuNP surface increases, this design places the RRM directly on the surface of the AuNP.[68] Recent work has shown that the analysis of samples in their dried state also plays an important role with respect to a consistency in the separation, and thus the plasmonic coupling, between the ERLs and the thin gold film used to form the capture address.[71, 72] We have shown that this approach is highly customizable and can be carried out using capture surfaces ranging from gold films coated on the bottom of the wells of microplates to arrays of glass-supported gold films with diameters of 200 μm for multiplexed applications.

Emergence of SERS Diagnostics

Early attempts to exploit the detection strengths of SERS as a quantitative analytical tool were hampered by an inablity to fabricate nanostructured materials (*e.g.*, roughened electrodes, nanoparticles, and various other architecutures) that would produce a consistant signal enhancement. [73-76] This inability reflected a

confluence of: (1) the extreme sensitivity of the enhancement on subtle differences in the architecture of the SERS-active surface; (2) the metastable nature of these materials with respect to oxidative, photochemical, thermal, and other processes (*e.g.*, Ostwald ripening and impurity adsorption); and (3) the technical gaps in past approaches of what we now refer to as bottom-up and top-down fabrication. Interestingly, many of these issues parallel those that complicate the fabrication of the atomically sharp tips required for the high spatial resolution capabilities of scanning tunneling microscopy (STM).[77]

As a result of delving more deeply into various fundamental aspects of importance to fabrication, recent work has begun to change this situation by enabling the reproducible preparation of nanoparticles and other nanostructures with well determined sizes and shapes for SERS applications.[78, 79] These developments include approaches to nanostructure stabilization by protective monolayer and polymer coatings or by silica, alumina, or other materials. [26, 80] Approaches using the increasing capabilites of inkjet printing and other fabrication tools are also becoming increasingly important.[81-83] This is not to say that all difficulties have been fully resolved, but rather that the understanding of approaches to their mitigation has now reached a level sufficient to energize investigations of SERS as a tool in the diagnostics arena.[68-70, 84-91] More to the point, recent developments have enabled many of the difficulties associated with realizing stable and reproducible measurements to be achieved on a case-by-case basis.

Equally critical to the application of SERS in the diagnostics arena is the ongoing revolution in spectroscopic instrumentation. Not long ago, SERS used bulky and costly

laboratory hardware (*e.g.*, high power lasers, triple monochromators, cooled detectors, and vibration isolators). Recent developments in compact lasers, optical filters, and array detectors have enabled the deployment of Raman spectroscopy in a number of previously inaccessible locations, including crime scene investigations and the industrial plant floor. These advances have also markedly reduced equipment and labor costs and improved ease of use (*e.g.*, the point and shoot modality realized by the adaptation of fiber optics as a carrier of the excitation light and an efficient collector of the scattered signal),[92, 93] while maintaining a high level of instrumental performance. The challenge now is to understand how SERS can meet the requirements of POC applications.

Application of SERS in Pathogen Detection

Illnesses caused by pathogenic agents (*e.g.*, bacteria, viruses, and fungi) account for nearly 20% of all deaths worldwide. **Table 1** lists several common infectious diseases, most of which are much more prevalent in developing regions of the world. With some diseases (*e.g.,* Hepatitis A), there are vaccines and sanitation measures that can drastically reduce the spread of the disease. However, we are beginning to see a resurgence of some diseases that were largely eliminated in many parts of the world due to failed immunization programs, the emergence of more serious co-infections, and more extensive global travel.

In addition to infectious diseases, SERS can be applied to the detection of biowarfare agents such as anthrax, ricin, and botulism. These agents have been organized into three classes by the U.S. National Institute of Allergy and Infectious Disease (NIAID) according to the severity of human responses and likelihood of the threat to exposure. Some examples are given in **Table 2**. Category A pathogens are

Table 1. Infectious Diseases Worldwide[94, 95]

Class/Disease/Pathogen	Type	Vector	% Total Death
Acute lower respiratory infections (Influenza, pneumonia, syncytial virus)	Virus	Shared fluids, airborne transmission	5.33
HIV/AIDS	Virus	Contact	2.78
Diarrheal diseases (*E. coli, Salmonella enterica, Listeria monocytogenes, Cryptosporidium purvum*)	bacteria, eukaryotic microbes, virus	Contact/ingestion	2.74
Tuberculosis	Bacteria	Shared fluids, airborne transmission	2.27
Malaria	Parasites	Mosquitoes	2.21
Meningitis	virus, bacteria,	Contact with respiratory secretions, contact with fecal matter	0.80
Hepatitis	Virus	Ingestion of contaminated food or water, close contact with an infectious person	0.58
Measles	Virus	Airborne disease, contact with saliva or nasal secretions.	0.24
Sexually transmitted diseases (excluding HIV; chlamydia, gonorrhea, and syphilis)	bacteria, viruses, parasites	Contact	0.22
Pertussis (whooping cough)	bacteria	Airborne disease, contact	0.15
Tetanus	bacteria	Puncture wounds	0.12

microbes that pose the highest risk to national security and public health because they can easily be transmitted from person to person and have the highest mortality rate (*e.g.,* anthrax). Category B and C pathogens are typically not as easy to weaponize for dissemination, may not be as readily available, and do not cause the magnitude of illness as Category A pathogens.

a. Biodefense applications. The world has become all too aware of the fact that pathogens can be packaged as biowarfare agents (BWAs) and can be disseminated by a range of methods. There are three types of BWAs: bacterial, viral, and molecular. BWAs are extremely difficult to detect in real time, can debilitating as well as lethal at very low exposures,[97] and can be delivered by unsuspecting postal/delivery services or by contaminated clothing, food, water, and companion animals. Regardless of delivery mode, the rapid and reliable identification of BWAs is a global security priority. This

Table 2. NIAID Pathogen Categories and Examples.[96]

Category	Description	Examples	Result of Exposure
A	Highest risk to national security and public health because they are: • Easily disseminated or transmitted from person to person. • High mortality rates. • Cause public panic. • Require special action for public health preparedness.	*Bacillus anthracis*	• Sores with black center (cutaneous) • Nausea, vomiting, fever, swollen neck (gastrointestinal) • Flu-like symptoms (inhalation)
		Clostridium botulinum toxin	• Difficulty swallowing or speaking, nausea, vomiting, trouble breathing, blurred vision
		Yersinia pestis (plague)	• Swollen lymph nodes (buboes), fever, headache, fatigue (bubonic) • Fever, abdominal pain, bleeding from mouth, nose, blackening and death of tissue (septicemic) • Cough, bloody sputum, fever, nausea (pneumonic)
		Variola major (smallpox)	• Fever, fatigue, headache, rash
B	Second highest risk because they are: • Moderately easy to disseminate. • Moderate morbidity rates. • Require specific enhancements for diagnostic capacity and enhanced disease surveillance.	Ricin toxin	• Fever, cough, difficulty breathing, tightness in chest (inhalation) • Vomiting and diarrhea, seizures, blood in urine (ingestion)
		Staphylococcus enterotoxin B	• Fever, headache, nausea, vomiting
		Cryptosporidium parvum	• Vomiting, watery diarrhea, fever
		Giardia lamblia	• Vomiting, diarrhea, fatigue
C	Third highest risk because they are emerging pathogens and may be developed in the future due to: • Availability • Ease of production and dissemination. • Potential for high morbidity/mortality rates. • Major health impact.	Influenza	• Fever, chills, cough, stuffy nose, fatigue, headaches
		Tuberculosis	• Persistent cough, pain in chest, blood in sputum, fever, fatigue, night sweats
		Rabies virus	• Fever, headache, weakness (initial) • Insomnia, confusion, partial paralysis (advanced)

section highlights a few of the many incisive studies that have taken advantage of the strengths of SERS in the design of new approaches to pathogen detection.

Ricin in Food. The detection of pathogens in food can be difficult due to spectral interferences (*e.g.*, background fluorescence[98]) from food matrices. Because of this, a sample preparation/extractive step is often needed. As an example, Labuza *et al.* have developed a SERS assay in which ricin B is extractively captured from orange juice and milk by an aptamer immobilized on an enhancing substrate composed of silver

dendrites.[99] Ricin, an NIAID Category B pathogen, is a naturally occurring lectin found in castor beans that disrupts cellular protein synthesis and can be lethal. It is composed of a toxic "A" and non-toxic "B" chain tethered together by a disulfide linkage. This study used a 5'-thiol DNA aptamer selective for the B chain. The aptamer capture layer (**Figure 3A**) was formed on the silver dendrite surface via thiol-silver chemisorption. SERS spectra for varying concentrations of ricin B spiked into phosphate-buffered saline (PBS; pH 7.4) were collected and analyzed using principle component analysis (PCA), which revealed that differences only weakly observable in the SERS spectra (**Figure 3B**) were much more notable after second derivative transformations (data not shown). Using this approach, *LoDs* of 50 ng/mL and 100 ng/mL were realized in less than 40 min for ricin B that was spiked into orange juice and milk samples, respectively, and then analyzed. Importantly, these *LoDs* are well below the amount of ricin that would be found in the volume of liquid a child would typically consume during a meal (~250 mL), given a minimum estimate of the LD_{50} of 1 milligram per kilogram of body weight and a child body weight of 20 kg.[100]

Anthrax in Human Serum. Anthrax is a U.S. National Institute of Allergic and Infectious Disease (U.S. NIAID) Category A pathogen. The most deadly form is

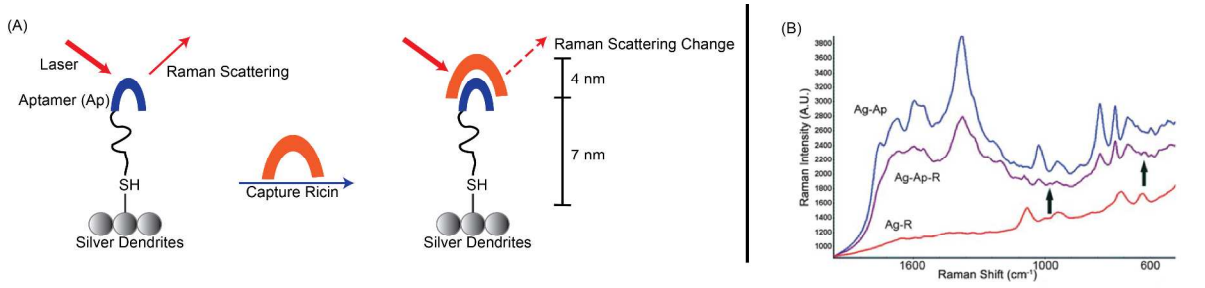

Figure 3. (A): Idealized representation of the "two-step aptamer SERS assay for ricin B. (B): SERS spectra for silver dendrite surface modified with aptamter (Ag-Ap), Ag-Ap surface after ricin B capture from PBS (Ag-Ap-R), and after direct deposition of Ricin B (Ag-R). Reproduced from Ref. 99 with permission from the Royal Society of Chemistry.

pulmonary anthrax, often leading to fatal respiratory collapse. In a recent study, a marker of the anthrax spore, poly-γ-D-glutamic acid (PGA), was detected in ~5 min at an *LoD* of ~100 pg/mL using an automated microfluidics construct, ERLs, and magnetic beads modified for selective PGA capture.[101] This *LoD*, obtained via ~~a~~ competitive immunoassay, is ~1000x below that of an ELISA experiment conducted in a side-by-side comparison. These studies, along with a peptide labeling strategy,[102] demonstrate the potential of SERS as a tool for the detection of pathogens central to biodefense needs. And, as discussed in the last section of this review, once SERS is fully integrated with a portable Raman spectrometer, field deployment should be possible.

b. Human health/infectious disease applications. There are several examples of moving SERS testing towards POC applications in human health care. This subsection highlights three sets of results: diagnostic tests for HIV, identification of respiratory viral infection (RVI), and detection of *Escherichia coli* (*E. coli*) strains responsible for urinary tract infection (UTI).

Detection of HIV gene sequences. Detection of DNA sequences from pathogenic agents by SERS has been an extremely active research area. Vo-Dinh *et al.* have designed a plasmonics-based silver nanoparticle (AgNP; 35-50 nm dia) assay that uses stem-loop DNA tagged with a rhodamine derivative that acts as a RRM in a molecular sentinel format. A molecular sentinel functions like a switch. In the absence of the DNA target, the hairpin configuration (closed state), keeps the RRM in close proximity to the AgNP surface and a strong SERS response is generated. When hybridized to its compliment target sequence, the extension of the resulting duplex positions the RRM beyond the enhanced electric field of the AgNP and the SERS signal is quenched (open

state).[103] The concept is illustrated in **Figure 4**. This test format has successfully been used to detect the *gag* gene sequence of human immunodeficiency virus type 1 (HIV-1) at a level on par with fluorescence-based detection and its versatility has since been demonstrated in assays for viral respiratory infections[104] and Dengue virus.[105] The next step in moving to POC is integration with easy-to-use approaches to sample preparation for utility in human serum and other key matrices.

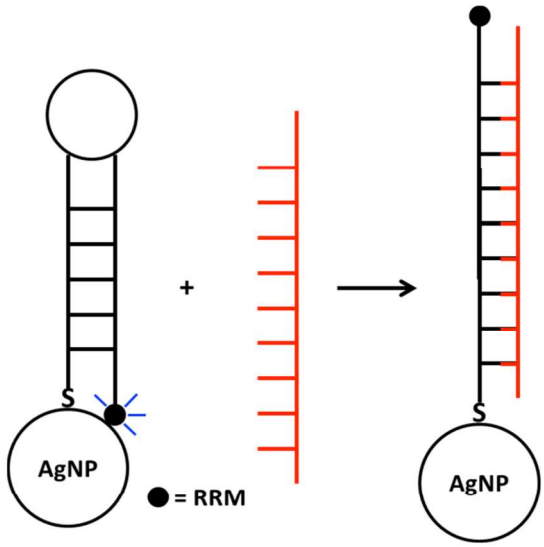

Figure 4. Concept for molecular sentinels (MS) using SERS. Adapted with permission from Analytical Chemistry, 2005, 77, 7810-7815, copyright 2005, American Chemical Society.

RVI. SERS has also found application in the identification of respiratory syncytial virus (RSV).[106, 107] This respiratory virus poses a serious health threat when infecting those with undeveloped or compromised immune systems (*e.g.*, infants and older adults). In this work,[106] Dluhy and colleagues applied oblique angle deposition (OAD) to fabricate silver nanorod arrays (~850 nm in length and 100 nm in diameter) to function as substrates with SERS enhancement greater than 10^8. This team used this architecture to measure the SERS spectra after the droplet evaporation for three different wild type RSV strains (A/Long, B1, and A2) and a G gene deletion mutant of the A2 strain. In contrast to the assay for ricin, the subtle spectral differences drawn out via principle component analysis (PCA) yielded a Scores plot that effectively discriminated the three wild type strains of RSV, but not the A2 strain from its gene-deleted mutant. This result is presented in **Figure 5**. However, when using hierarchical

cluster analysis (HCA), dendrograms generated via K-mean classification enabled the reliable identification of all four targets. This work indicates that molecular fingerprinting by SERS can differentiate closely related strains of RSV as well as DNA sequences of RSV with a single gene mutation. Moreover, this readout detected these markers at ~10^3 plaque-forming units (PFUs), which is ~20x below that for ELISA.

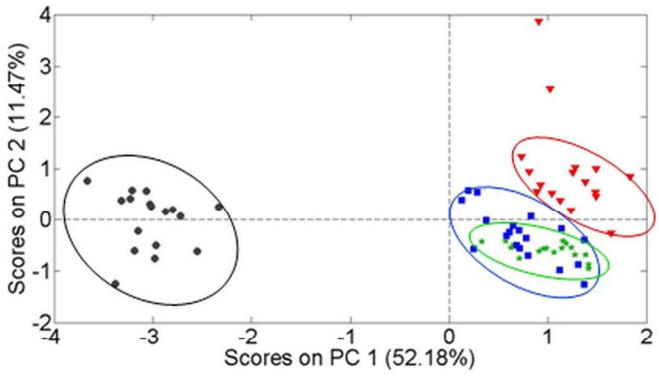

Figure 5. PCA Scores plot of PC2 vs. PC1 computed from the SERS spectra of the RSV strains A/Long (●), B1 (▼), A2 (■), and the recombinant strain A2 G gene deletion mutant (★). *Reproduced with kind permission from Analytical and Bioanalytical Chemistry, "Identification and Classification of Respiratory Syncytial Virus (RSV) Strains by Surface-enhanced Raman Spectroscopy and Multivariate Statistical Techniques", 2008, 390, 1551-1555.*

UTIs. UTIs are one of the most common types of bacterial infections, particularly in women. There is 20% chance that a woman will have a UTI in her lifetime, with 20% of those having been infected once of becoming infected again.[108] Today's gold standard test for UTIs uses a quantitative urine culture that has a turn-around time of 24 h. A count of 10^5 or more colony-forming units per milliliter (CFUs/mL) stands as the cutoff for a UTI-positive result. An additional 24 h is needed to complete tests for antibiotic susceptibility.[109, 110] In an effort to reduce turn-around time while maintaining clinical accuracy, the use of SERS as a diagnostic test using urine specimens was investigated by Pitris and coworkers.[109, 110] For this purpose, dilutions of two strains of *E. coli* in filtered urine were mixed with equal volumes of silver nanoparticles, the resulting suspensions were spotted and dried on glass slides, and SERS spectra were collected. The results show that the presence of the two *E. coli* strains can be quantified

by integrating the peak intensity in the C-H stretching region (2900-3000 cm^{-1}) down to a level of ~10^3 CFUs/mL, which is well below the true positive cutoff of 10^5 CFUs/mL. This work also demonstrated that SERS, when used in combination with PCA, can evaluate antibiotic susceptibility for treatment with amoxicillin and ciprofloxacin.[109, 110] Pending the results of validation studies with urine specimens from infected patients and healthy controls and efforts to concentrate specimens by ~100x via filtration, this development has the potential to challenge culturing as the standard for UTI testing**.**

c. Food/Water security applications. Safeguarding the global food and water supply is one of this century's most significant challenges. Recent reports estimate that in the U.S. alone there are more than 48M foodborne illnesses each year[111] with an associated economic burden approaching $77B USD.[112] However, the ability of regulatory agencies and public health authorities to protect these critical resources is severely compromised by the lack of tests that can be applied on-site and have a short-turn-around time. This difficulty is compounded by the fact that foodstuffs come in different physical forms (*e.g.,* liquids and semi-solids) and compositions (*e.g.*, varied levels of proteins, carbohydrates, fats, and indigenous microbes), which can demand unique approaches to sample collection/preparation. In fact, these are precisely the limitations which led to the emergence of the costly test-and-hold policies (while awaiting test results) used today in many parts of the food industry.[113]

Pathogens in Food. One intriguing SERS approach to detecting microbes on the surface of edibles uses a separation step that is followed by selective target tagging by AuNPs designed along the lines of ERLs.[114] **Figure 6** shows the key steps in the process. The first step separates the target from the food matrix with magnetic

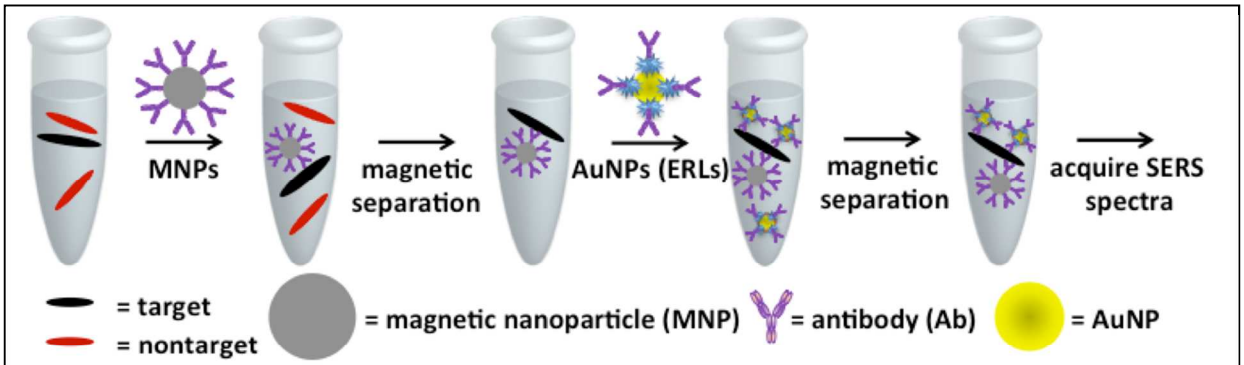

Figure 6. Approach (not scaled) to the magnetics-based separation and SERS detection via modified AuNPs. Adapted from reference.[89]

nanoparticles (MNPs) surface-modified with antibodies specific to the target. The MNPs have a Fe_3O_4 core, which is encapsulated with a silica layer that is capped with amine groups in order to tether Abs to the silica surface after gluteraldehyde treatment. The post-processed diameter of these particles is ~100 nm. The next step incubates the functionalized MNPs in a liquid matrix spiked with *Salmonella enterica* (*S. enterica*) senovar Typhimurium, a pathogen commonly associated with food poisoning. These test samples were prepared by adding freshly washed spinach leaves to PBS that was then incubated at 37 °C for 3 h after spiking with *S. enterica* senovar Typhimurium. MNP incubation selectively extracts the pathogen from the sample by means of antigen-antibody binding and is followed by a magnetics-based isolation process, washes with PBS, and a final resuspension in PBS. The analysis is completed by incubating the MNP suspension with AuNPs, a second magnetics isolation, washes and resuspension steps, and SERS readout. In this work, the ERLs are prepared by forming a mixed monolayer of the RRM 4-mercaptobenzoic acid (MBA), which is an inherently strong Raman scatter, and an Ab, which is specific for the target. These measurements gave an *LoD* of ~10^3 CFU/mL for *S. enterica* senovar Typhimurium and, in a parallel study, a comparable *LoD* for the detection of *Staphylococcus aureus* spiked in the same extract.

Others have used SERS to identify *Listeria monocytogenes* in milk[115] and metabolytes of vitamin D_3 in spiked human serum.[116] Interestingly, a recent study has proposed procedures, backed up by experimental results, to potentially introduce Raman scattering as means to improve today's standard food testing requirements per the International Organization for Standardization (ISO).[117]

Pathogens in Environmental Samples. In addition to scrutinizing the food supply, Raman scattering has potentially found a place in screening for waterborne pathogens. Rule and Vikesland have developed a method that uses surface-enhanced resonance Raman scattering (SERRS) for the rapid detection of *Cryptosporidium parvum* (*C. parvum*) and *Giardia lamblia* (*G. lamblia*).[118] SERRS combines the signal amplification from the optical resonance of chromophores (*e.g.*, dye molecules), which is the basis of resonance Raman scattering, with that from the plasmonics-based enhancements of the electric field central to SERS. These protozoan pathogens cause gastrointestinal illnesses that can have a serious health effect on individuals with compromised immune systems, but are not effectively inactivated by common drinking water disinfectants. More to the point, the methods standardized, for example, by the U.S. Environmental Protection Agency (EPA) are tedious, require a high level of expertise, and have poor analytical recoveries. This work prepared ERLs using AuNPs (40 nm dia) modified with either the RRM malachite green isothiocyanate (MGITC) followed by conjugation with *G. lamblia* Abs or with the RRM rhodamine B isothiocyanate (RBITC) followed by *C. parvum* Abs. SERRS measurements were made after fixing the protozoa on glass microscope slides, incubating with 5% bovine serum albumin (BSA) to minimize nonspecific adsorption, and treatment with the corresponding ERL suspensions.

A result from this study is given in **Figure 7** as SERRS intensity maps across small sections (~10 x 10 μm) of the glass substrate. **Figure 7A** is a map of the phenyl-N stretch (1618 cm^{-1}) of the ERL prepared using the RRM MGITC in tagging *G. lamblia* cysts, whereas the map in **Figure 7B** is that for the ring C-C stretching vibrations (1645 cm^{-1}) of the ERL fabricated with the RRM RBITC for tagging *C. parvum* oocysts. Bright field microscopy was used to locate the targets on the sample prior to SERRS mapping and gave images consistent with the shapes and sizes of the two different pathogens (*e.g.*, ovoid shaped *G. lamblia* cysts and spherical *C. parvum* oocysts). The dashed line in the SERRS maps outlines each organism. As evident, the signal distribution is more varied across the *G. lamblia* cyst than the *C. parvum* oocyst. This was found to be a consequence of the weaker signal generated by using MGITC as an RRM, which was confirmed by a marked improvement in signal uniformity when switching to RBTIC. To test clinical accuracy, 20 oocysts and 20 cysts were tagged with a suspension containing both sets of ERLs and by averaging the SERRS signal at three locations on the surface of an oocyst and six locations on the surface of a cyst. A true positive response was assigned to a SERRS response that was collocated within the dashed region of the map. In contrast, a signal was ascribed to a

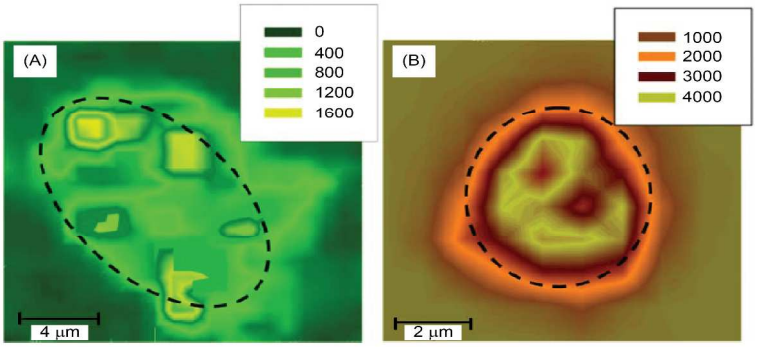

Figure 7. SERRS *x-y* maps of: (A) *G. lamblia* cyst and (B) *C. parvum* oocyst. The dashed line outlines the organism. The map of the *G. lamblia* cyst is the intensity of the 1618 cm^{-1} peak (MGITC), whereas that for the *C. parvum* oocyst is 1645 cm^{-1} peak (RBITC). Mapping settings: (A) 20 × 20 measurements in 1 μm steps and 1 s acquisition times. (B) Mapping settings: 10 × 10 measurements with 1 μm steps and 1-s acquisition times. The intensity color scales are in counts per second. *Reprinted with permission from Environmental Science and Technology, 2009, 43, 1147-1152, Copyright 2009, American Chemical Society.*

false positive response if located on the incorrect organism. This test gave sensitivities and specificities for C*. parvum* of 100% and 85% and for *G. lamblia* of 100% and 100%, respectively, clearly demonstrating the identification and differentiation power of this test format. To move forward, the next steps will focus on the design of a filtration method to collect/concentrate waterborne pathogens and to validate performance using water samples collected from field sites.

d. Veterinary medicine. In addition to the obvious implications to biodefense and global food and water supplies, the need for improved animal health care tests reflects the soaring companion animal population in the past 20 years.[119] Estimates suggest the United States spent close to $15B USD on companion animal care in 2014.[119] One example where SERS has proven advantageous in animal health is the low-level detection of the bacterium *Mycobacterium avium* spp. paratuberculosis (MAP), the causative agent of the bovine wasting disease known as Johne's disease, a contagious and fatal gastrointestinal disorder that leads to nutrient malabsorption. The early detection of MAP, however, is difficult. Animals do not become symptomatic until a few years post infection, which can result in the spread of the disease across a herd. When diagnosed, the herd is usually destroyed to halt disease spread. The current test for detecting MAP infection is fecal culture. Culture tests can cost upwards of $40/sample USD and, since MAP is a "slow grower," can take 4-5 weeks.[120]

Our[121, 122] and other[123, 124] laboratories have explored improvements to screening cattle for MAP, adding that MAP has recently been implicated as a possible agent for Crohn's disease in humans.[125] **Figure 8** presents the results for the SERS immunosorbent assay where MAP in whole milk is the target and includes a set of

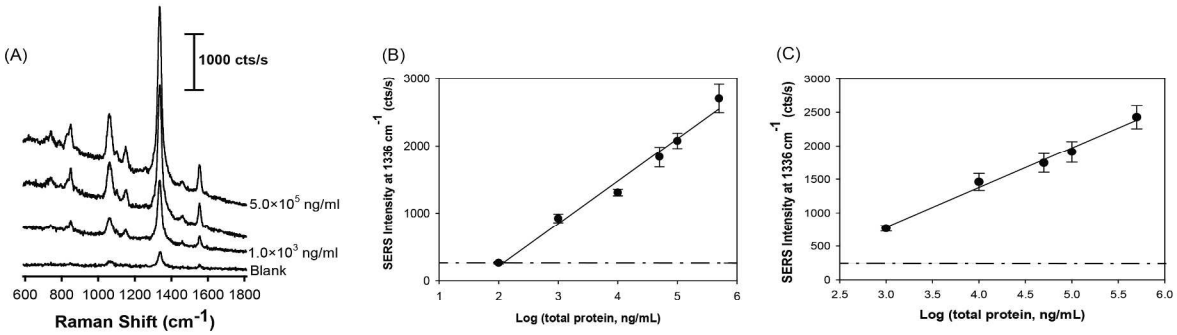

Figure 8. Spectra and calibration curve for sonicate-spiked PBS and milk samples. (A) Spectra (vertically offset for clarity) for sonicate in PBS. (B) Caibration curve in PBS. (C) Calibration curve for sonicate in milk. Dashed lines correspond to the blank plus three times its standard deviation for each matrix. *Reproduced with permission from Clinical and Vaccine Immunology, 2008, 15, 227-234.*

spectra and calibration curves for sonicates of MAP spiked into PBS and whole milk. These results were achieved in less than 24 h and at an estimated cost of ~$2/sample. In applying the approach described above to detection of MAP in milk samples, we have been able to achieve an *LoD* of 200 ng/mL, which translates to ~1000 MAP cells/mL.

Shifting the Paradigm towards SERS POC Diagnostics

As noted, to responding to a possible public health emergency places a premium on the performance of diagnostic tests. Today's tests, however, lack the ability to identify the causative agent of a potential threat in a timely manner due to a combination of factors, including lengthy assay steps, the need for sample pre-processing, and the development and cost of field-ready test kits and hardware.[53] Moreover, early detection ideally requires a test with a high clinical sensitivity and even higher clinical specificity to attain a clinically actionable positive predictive value.[126, 127] In this regard, conventional markers when used in a univariate (singleplex) format often perform poorly.[128] As a result, the identification and validation of multiple markers to realize a "pathogen signature" has become a cornerstone in the design of emerging tests.[129-135] The use of

SERS-based methods holds promise for POC diagnostics due to improved *LoDs*, multiplexing capabilities, ease of use, and cost effective instrumentation.

In completing this review, the last sections examine a few of the obstacles that must be overcome for SERS to become part of the toolbox for the next generation of diagnostic tests. These include an overview of the attributes of an ideal POC test, a discussion of key performance metrics of a diagnostic test from both chemical and clinical analysis points of view, and a perspective on the steps to transition a SERS-based diagnostics platform from the R&D laboratory to the POC arena.

Attributes for an ideal diagnostic test. Having highlighted only a small portion of the seminal work on SERS for pathogen detection, this section examines the challenges faced in moving to POC diagnostics. We start by examining the attributes of an ideal diagnostic test as specified by the "ASSURED" criteria recently put forth by the World Health Organization (WHO)[136] (**Table 3**). ASSURED reflects the fact that clinical laboratories in developing countries are often poorly resourced and that cost, lack of robustness, and ineffective performance due to high ambient temperatures and other environmental factors compound the difficulties in POC deployment.

The ideal POC diagnostic platform has several key attributes. First, and perhaps most important, it needs to be self-contained and easy to use. In remote areas, POC technologies that rely on data uploading and remote analysis/interpretation may be limited due to inadequate communication network availability. Further, it is not always possible to have highly-trained medical personnel present to perform sophisticated tests. A second aspect is cost. Commercial POC diagnostics for a large number of markers are available, but either the tests or readout tools are cost-prohibitive for

Table 3. Descriptors and characteristics of the WHO's ASSURED attributes for ideal POC test.

Attribute	Descriptor	Comments
Affordable	Test affordable by those at risk	Cost per test must match 1-2 days of income
Sensitive	Few false negatives	High true positive rate insures that those not infected are not treated
Specific	Few false positives	High true positive rate identifies only those needed treatment
User friendly	Easy to use	Requires only a few simple steps and minimal operator training
Robust and rapid	Short turn-around-time (~30 min), long shelf life (>1 year) of regents	Enable treatment in same visit to care giver
E: Equipment-free	Compact, battery powered unit	Readily transportable
Deliverable where needed	Portable, hand-held, cloud-enabled	Few consumables, little waste

widespread deployment in resource-limited settings. Cost can, however, be lowered by multiplex testing. Finally, it is important to consider portability. While the "E" in ASSURED stands for equipment free, it is likely that the near term solutions for POC, will be rugged, battery-powered instrumentation with a weight conducive to easy transport to remote areas. As evident, the development of an ASSURED diagnostic test is a formidable task, but one that should be reachable for SERS with the new generation of field portable Raman spectrometers entering the marketplace.

b. Figures of merit. To set the stage for transitioning a test from the R&D laboratory to POC, there are a few key, but often overlooked, distinctions in definitions that should be made between the statistics of analytical measurements and those central to the clinical accuracy of a test. Foremost are the metrics of analytical and clinical performance, which are summarized in **Table 4**, along with typical acronyms. These metrics include those common to chemical analysis [*i.e.*, limit of blank (*LoB*) limit of detection (*LoD*), limit of quantification (*LoQ*), analytical sensitivity (S_A), and quantitative resolution (Q_R)] and those central to clinical accuracy [*i.e.*, clinical sensitivity

Table 4. Definitions of Performance Metrics[a,b]		
Metric	Definition	Mathematical Expression
Limit of blank (*LoB*)	Measurement level for blank sample	$LoB = 1.645\sigma_0$
Limit of Detection (*LoD*)	Response of sample with sufficient target to be distinguished from the blank at a predefined confidence level	$LoD = LoB + 1.645\sigma_D \rightarrow 3.29\sigma_0$
Limit of Quantitation (*LoQ*)	Response of sample with more than sufficient target to unambiguously be a true positive	$LoQ = 10\sigma_0$
Analytical Sensitivity (S_A)	Change in response with change in concentration of target	$S_A = \frac{dR}{dC}$
Quantitative Resolution (Q_R)	Measure of ability to differentiate the response at one target concentration from that at different concentration	$Q_R = \frac{\epsilon_R}{S_A}$
Clinical Sensitivity (C_{sens})	Fraction of infected patients correctly identified by the test as being infected	$C_{sens} = \frac{TP}{(TP + FN)} \times (100)$
Clinical Specificity (C_{spec})	Fraction of healthy patients correctly identified by the test as being healthy	$C_{spec} = \frac{TN}{(TN + FP)} \times (100)$

a. Normal distributions, null hypothesis ($\sigma_B \rightarrow \sigma_0$), $\sigma_0 = \sigma_B = \sigma_D = \sigma_Q$, and α = β = 0.05, 95% confidence levels.
b. TP is the number of true positive tests; FN and is number of false negative tests; TN is the number of true negative tests; and FP is the number of false positive tests. ϵ_R is defined by the uncertainty in the measurement.

(C_{sens}) and clinical specificity (C_{spec})]. Chemical analysis metrics characterize the performance of the analytical measurement. Clinical metrics quantify the accuracy of a test result with respect to whether a patient is or is not infected with a given disease.

There are two main governing bodies, the Clinical and Laboratory Standards Institute (CLSI)[137] and the International Union of Pure and Applied Chemistry (IUPAC), charged with applying scientific rigor to these definitions.[138] As detailed shortly, one of the overlooked issues develops from one of the often used definitions of *LoD*[139] and how it applies to an assessment of clinical accuracy. As a starting point, this section briefly reviews the definition and interpretive value of these metrics to a univariate system, and is followed by examining how they relate to clinical criteria for treatment, and a perspective on when multivariate analysis is needed.

Chemical Analysis Metrics. These metrics apply only to measurements in which the error is purely random.[140] If such a measurement is repeated a sufficiently large number of times, the results will be symmetrically distributed about the average or mean

($\overline{x}$) concentration of the target in a sample. The width of this Gaussian curve (**Figure 9**) characterizes how tightly the data clusters about $\overline{x}$ and is quantified by the standard deviation, *s*. As the number of measurements increases, *s* approaches the true standard deviation of the distribution, σ, and $\overline{x}$ approaches the true mean, μ, of the distribution.

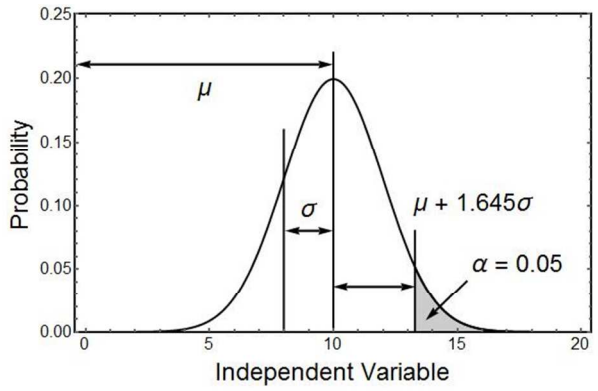

Figure 9. Plot of a Gaussian curve centered at the true mean, μ, with a true standard deviation, σ. The position at $\mu + 1.645\sigma$ corresponds to $\alpha = 0.05$, which means for the one-tailed test shown that 95% of the distribution is below $\mu + 1.645\sigma$ and the shaded region represents the remaining 5% of the distribution.

The *LoB* is the largest apparent concentration likely to be observed in replicate blank samples. Since the blank is devoid of target, it is a measure of instrument noise, experimental bias, and other errors. In an immunoassay, nonspecific adsorption is a common contributor to blank measurements. Ideally, blank samples should have the same matrix composition as the test samples.[137, 141] Per **Table 4**, the *LoB* is the response that is greater than 95% of those in the blank distribution, where μ_B and σ_B are the mean and standard deviation of the blank distribution, respectively. The value at $1.645\sigma_B$ is the response above 95% (α = 0.05) of the probability distribution. Note that responses in the upper 5% tail of the distribution are greater than the *LoB* and

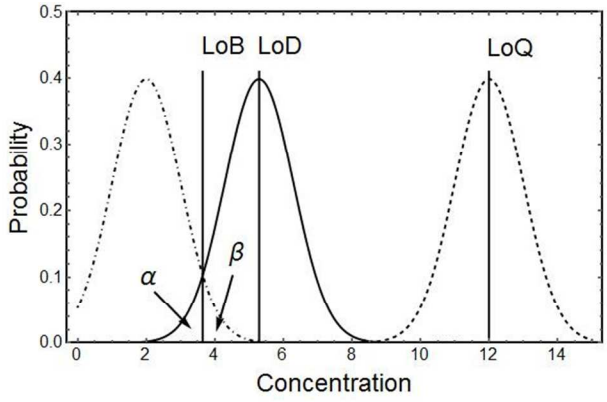

Figure 10. This figure shows the IUPAC definitions of limits at the recommended parameters of α = β = 0.05, and RSD = CV = 10%. α corresponds to the fraction of false negatives and β corresponds to the fraction of false positives. In this plot, a bias of 2 units was applied to the blank and $\sigma_0 = 1.0$ for an $LoB = 2.0 + (1.645\sigma_0)$, $LoD = LoB + 1.645\sigma_0$, and $LoQ = 2.0 + 10.0\sigma_0$.

represent false positives. **Figure 10** gives an example of the distributions and limits for this and the following discussion.

The *LoD* is the lowest concentration that can be statistically distinguished at a 95% confidence limit from the *LoB*. That is, 95% of the measurements lie above the *LoB*. In this case, 5% of the distribution of the sample measurements fall below the *LoB* (β = 0.05) and would represent false negatives. The *LoQ* is a more functional metric with respect to the quality of the result. It is the response that is ten times greater than the standard deviation of the sample measurements, σ_o.

Given the intertwined nature of *LoB*, *LoD*, and *LoQ*, the only way to lower the *LoD* is to tighten the blank distribution and/or reduce the background signal. Both are often linked to combatting non-specific adsorption. Conversely, if the mean of the sample response can be increased to a value well above the blank distribution, the impact of the *LoD* becomes less important. This creates a clear delineation between the blank sample distribution, eliminating false positive and false negative responses.

This analysis also applies to a test which measures the level of a marker that may be up- or down-regulated due to disease onset. In this case, the ability to use a marker depends on the difference in its distribution in healthy and infected patient populations. This treatment follows the statistical approach applied in **Figure 10**, recognizing that the distribution given for the blank samples now corresponds to that of the healthy population when a marker is upregulated with disease onset and that the most effective cutoff between true positive and true negative results entails receiver operating curve (ROC) analyses.[142, 143]

The ability to discriminate between two patient populations is dependent on analytical sensitivity (S_A)[138, 144] and quantitative resolution, Q_R. S_A quantifies the rate of incremental change in the response, *dR*, in a measurement with respect to an incremental change in concentration, *dC*. It is the instantaneous slope of a calibration curve. Moreover, Q_R is defined by S_A and the uncertainty in the measurement, ϵ_R, as given in **Table 4**.[144] Q_R measures how well the responses at two different concentrations can be distinguished from each other. In **Figure 11**, the error in the response is held constant, translating to different absolute errors being mapped onto the input (*e.g.,* concentration) axis. Clearly, the higher slope of curve A enables the determination of smaller differences in input than curve B. For diagnostic tests, this improves the detection of small changes in concentration and therefore enhances the ability to track changes in response to treatment.

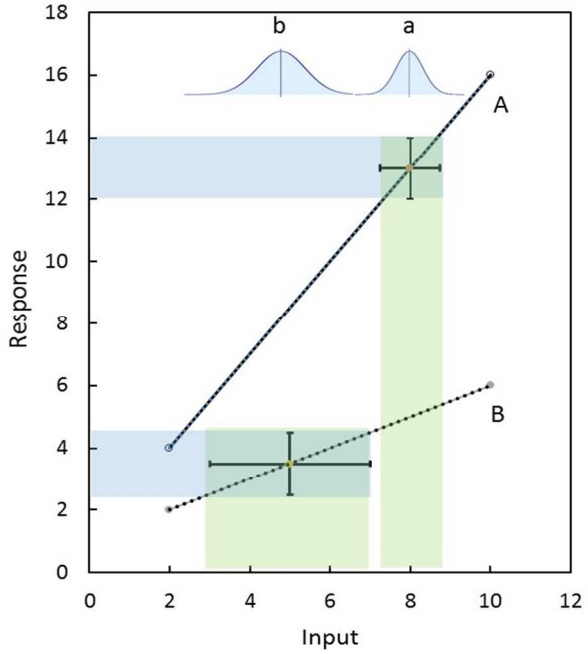

Figure 11. Illustration of analytical sensitivity and quantitative resolution, assuming a fixed error of one unit in the response. The analytical sensitivity (slope) determines the input range within the response error. As the slope decreases, the input range increases, which will give a response within the response error. The Gaussian distribution plots represent the input distributions for the two slopes in order to depict the resolution in input that will be possible (how close can input values can be to each other and still be statistically distinguished.) [Line A: $y_A = (1.5)x_A+1.0$, Line B: $y_B = (0.5)x_B+ 1.0$].

Returning to the commonly used analytical chemistry definition of *LoD*,[139] the often used "signal detection limit", which is at $3\sigma_B$ above the mean signal of the blank, is comparable to the IUPAC definition. Using this definition, ~50% of the measurements of

a blank sample will appear to have a detectable level of analyte, whereas 50% of the measurements of a sample containing analyte will appear to be devoid of target. Yet another definition of *LoD* is set at $3\sigma_B/m$ where *m* is the slope of the calibration curve, which adds another level of analysis complexity. Nonethless, the CLSI definitions in **Figure 10** separates the health and infected patients distributions in a manner that is more effective in terms of a predictibale measure of clinical accuracy.

The metrics used for chemical analysis are extremly important in the analysis of SERS substrates due to the questions that surround the quantifiability of SERS substrates caused by variations in the signal due to its distribution across the substrate and disparity between substrates. Careful consideration of analysis methods and sample preperation are important in the production of SERS-based methods.

Clinical Analysis Metrics. The true value of a diagnostic method is determined from the results of an evaluation of patient samples, which are used to quantify C_{sens} and C_{spec}. C_{sens} and C_{spec} are connected to the *LoB* by the statistical distributions of the response for healthy and infected patients in that the degree over the overlap of the two distributions determines the expected number of false negatives and false positives.

C_{sens} represents the proportion of true positives (*TPs*) correctly identified as such. It equals the number of true positives divided by the total number of infected people. The total number of infected people is equal to the sum of the number of true positives plus false negatives (*FNs*). Statistically, if the tested patient pool is composed of 100 healthy and 200 infected individuals, then using the defined limits of detection (α = β = 0.05 for *LoB* and *LoD*), there would be 190 true positive test results and 10 false negative test results, which equates to a C_{sens} equal to 95.0%.

On the other hand, C_{spec} is determined by the proportion of true negatives (*TNs*) correctly identified as such. It equals the number of true negatives divided by the total number of healthy people. The total number of healthy people is equal to the sum of the number of true negatives plus false positives (*FPs*). Using the earlier example there would be 95 true negative tests and 5 false positive tests or a C_{spec} of 95.0%.

To increase C_{sens} and C_{spec} beyond the defined maximums per the *LoB* and *LoD* definitions, the overlap between the sample and blank distributions must be reduced. Indeed, the *LoQ* definition of IUPAC will always separate the blank and sample distributions sufficient to give theoretical C_{sens} and C_{spec} values approaching 100%.

Clinically, the region of overlap between healthy and infected distributions may require alternate decisions on cutoffs based on the nature and treatment of the disease. For example, for a disease that is treatable but with serious consequences if not treated, the analysis may be designed to skew the return to more positive responses and therefore acceptance of the risk of treating uninfected patients. Some thresholds may aslo be constructed to signal the possibility of an infection, but be more indicative prescribing a retest in the near future to gage the liklihood of progression.

Several SERS-based diagnostic methods have progressed to the stage where patient samples have been analyzed.[145-148] The true merit of these tests is determined by the correct identification of healthy and infected patients based on the analysis of patient samples, which are then compared to a gold standard test to validate the clinical accuracy of the new test. However, a reasonably large set of positive and negative samples are needed to correctly determine the C_{sens} and C_{spec} of the method.

Multivariate Analysis. Multivariate analysis (MVA) is important in tests involving

the simultaneous measurement of multiple disease markers with signal overlap, when a target has no identifiably distinctive spectral feature from that of the sample background, or when there is signal interference.[149] MVA spans a number of approaches to data analysis based on pattern recognition, and includes principle component analysis, principle components regression, partial least-squares, stimulated annealing, and neural networks.[150, 151] In general, MVA involves the analysis of a number of different spectral features by using algorithms that identify the natural variance in the data or by means of partial least squares (PLS) regressions or artificial neural networks that are guided by *a priori* knowledge of the samples under investigation. These variances define the magnitude of a set of basis vectors, which are constructed from the spectra of a large set of standard samples. At this point, the vector of the unknown can be projected onto an orthogonal set of the basis set of vectors known as principle components. Typically, the largest orthogonal vectors are applied to construct “score” plots, which are two dimensional slices of the vector space that represent the contributions from each component in distinct areas of the plot. Building signal-to-concentration correlations into the model allows quantified results to be extracted from the unknown spectrum.[152-154] [155, 156] [149, 150, 157-160] As expected, the quality of the result is strongly linked to “training data set” in terms of matching the unknown samples.[155, 161]

Lastly, when attempting to detect a target without a identifiably distinctive spectral feature, as has occurred in the SERS analysis of cell cultures, then building a partial least squares discriminant analysis model based on cell concentrations of a pure culture can be used as a means to quantify the target in an unknown sample. A recent example of this approach examined the determination of the pathogen *Mycoplasma*

pneumoniae by a partial least squares algorithm.[162] The results indicated the ability to detect target DNA at a level on par with that of qPCR, ~5 genome equivalents/μL.

Moving a Diagnostic Test from the R&D Laboratory to POC

The path to the development of a new diagnostic testing technology has several stages, for which a general overview is given in **Chart 1**. This chart and the discussion that follows highlight many of the challenges typically faced in each development stage, along with a few more specifically related to SERS-based detection platforms. **Stage 1** begins with an innovation, which is often the result of curiosity-driven research. For example, our interest in diagnostics came about when members of my research group proposed that the surface modification and analysis tools we had been developing to

Chart 1. Stages of Diagnostics Test Development.

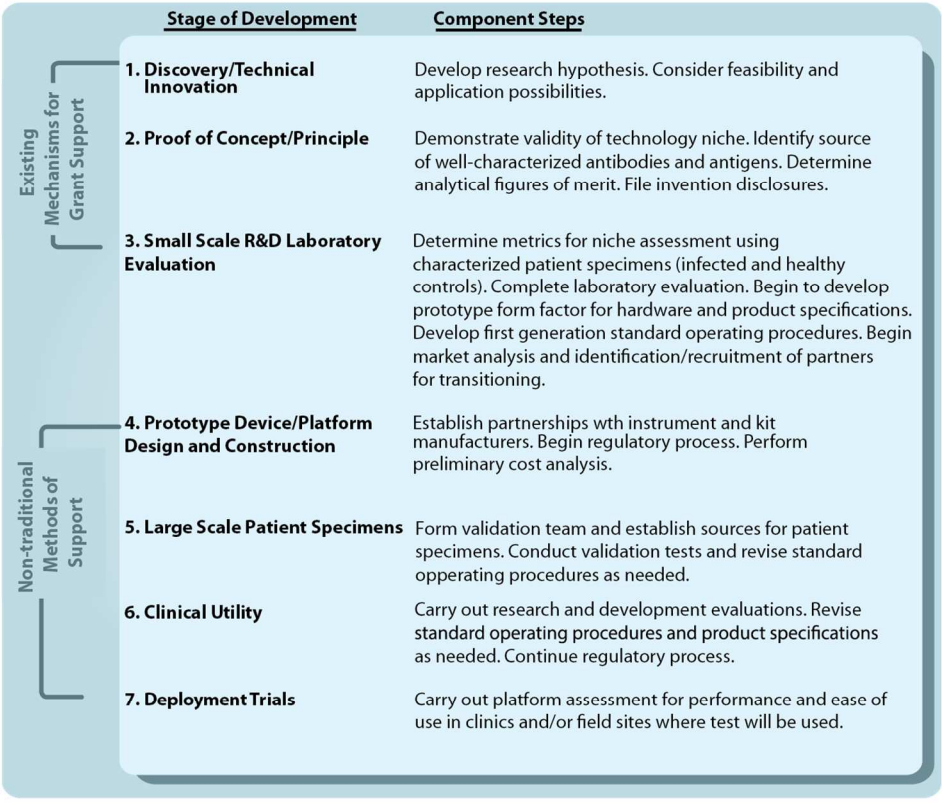

study the fundamental underpinnings of reactions and processes at interfaces (*e.g.*, electrocatalysis, friction, and wear) may have applicability in bioanalytical chemistry.

Not surprisingly, the most problematic attributes in **Table 3** that continually challenge the diagnostic testing landscape are clinical accuracy, cost (hardware and per test), robustness, repeatability, turnaround time, and ease-of-use. The principle focus of **Stage 2** is therefore to assess, via proof-of-concept studies, how an innovation potentially addresses these issues. That is, **Stage 2** should focus on obtaining preliminary data that documents the potential of the new test to supplant an existing technology or to realize a new capability. Most SERS-based development efforts at **Stage 2** aim at determining if the innovation can redefine the *LoD* for a marker, reflecting the assumption that improvements in the ability to detect a marker earlier in the progression of a disease will translate into more favorable patient outcomes. Efforts focused on the concurrent detection of multiple markers for a pathogen represent an important variation of this theme.

The challenge most often faced with SERS at **Stage 2** is development of a fabrication process that can repeatedly form nanostructured materials with a consistent signal enhancement. This challenge distills to a clear statement of the required level of reproducibility. Many commercial tests (*e.g.*, ELISA) report a relative reproducibility of ~15% or better. While reproducibility has been a major obstacle in the past with SERS, recent work has begun to overcome the challenges in measurement reproducibility through the development of approaches for the reproducible construction of plasmonic architectures.[76, 163] In our case, this involved establishing an in-house procedure to “size qualify” the AuNPs that serve as the core structural element in our ERLs.[36] And, as will

be reported elsewhere, we have developed optical methods that allow us to quantify the reproducibility in forming the Ab and RRM layers that coat the ERLs.

Stage 3 continues to focus on demonstrations that document ability of the new test to gain a foothold in the marketplace, and may entail tackling manufacturing challenges and costs, refining experimental protocols to improve ease of use, or establishing the effectiveness of the test by running a small number of patient or type of realistic samples. It is here that momentum can stall due to an inability to establish a clear technical advantage and/or competitive cost basis over existent methodologies. Indeed, we are often asked to estimate a per test cost by those interested in the commercialization potential of SERS due to the use of gold as the signal enhancing architecture. Like most immunoassays, however, antibodies are the most expensive component of our test platform. Nonetheless, seeking input from or forming partnerships with experienced instrument and/or kit manufacturers will provide a much more effective route to addressing cost concerns.

Up through **Stage 3**, most of the work can be supported by traditional mechanisms, including small business research grants and innovation-based support opportunities. **Stages 4-6,** however, will require much more significant levels of resources, including a large, multiyear financial investment, and a much broader and more diverse range of technical and clinical expertise of the product development team. There are no orchestrated paths on how to move forward at this point, but several government agencies and other organizations now exist that may serve as useful resources. Again, engaging end users (*e.g.*, clinicians and hardware and tests kit manufacturers) and other experts (*e.g.,* biostatisticians) at this stage will enhance

likelihood of success. These experts will prove invaluable in the selection of markers that are robust in terms of their correlative value with the identity of the pathogen or infectious disease and in identifying and resolving issues related to sample collection, preparation, operator safety, and waste disposal.

Stage 4 (Prototype device/platform design and construction) starts with an in depth engineering and manufacturing study to transition the footprint of the R&D platform to one with attributes sought for the targeted application. These considerations include how to reduce size, weight, and power requirements, while maintaining the needed performance capabilities of the R&D system. This stage should also address any issues related to the temperature of the environment proposed for deployment and possible difficulties with respect to the cold chain (*e.g.*, kit/reagent stability vis-à-vis a well maintained temperature-controlled supply chain). This is also a good time to begin to work on methods standardization, market analysis, and, where applicable, to begin any regulatory requirements. For SERS, these design issues should include the impact of temperature and other possible environmental issues with respect to laser power and stability and how to design a small sized spectrometer with high light collection efficiencies and high stray light rejection.

Stage 5 (Large-scale validation) has a number of components and often proceeds in parallel with **Stage 4**. A key element of **Stage 5** involves determination of the number and types of samples required for statistical relevance; collaborators in biostatistics can aid in establishing data analysis strategies and in refining the overall approach to quantifying clinical accuracy. To complete these phases of development, it is important to establish assay procedures that have as simple as work flow as possible.

These procedures must also be designed to avoid any preanalytical bias and analytical bias. Preanalytical bias can arise from systematic differences in patient populations, sample characteristics, and procedures used for sample collection, handling, and storage. This type of bias can be managed and minimized by carefully defining the focus of the test which will aid in the inclusion and exclusion of patient specimens based on assessments of sample and patient histories. To minimize or control the repeatability of the bias, this process should also include metrics and standard operating procedures (SOPs) for sample collection, handling, and storage, and measurement and documentation of all potential sources of uncontrollable variation.

Analytical bias, on the other hand, is due to systematic errors in a procedure and can be corrected by extensive training, exacting performance measures for instrumentation, and use of SOPs. For SERS, SOPs should also include measures to ensure the reproducible fabrication of the plasmonic contributors to the assay (*e.g.,* the size and shape of the AuNPs). Plans and procedures should also be put in place with respect to consistent data analysis, record keeping, and data archiving. There is one particular problem to note: antibody and antigen consistency. Both pose well-recognized difficulties in the eventual adoption of a new test by end users, and the reader is referred to several insightful discussions on mitigation.[164, 165]

Stage 6 (Clinical utility) and **Stage 7** (Deployment trials), can run concurrently with **Stages 4** and **5**. Clinical utility has been identified as a separate stage because it includes an in-depth assessment of how the new test would fit in the workflow in a clinical facility or be effectively deployed for field work vis-à-vis POC. Both of these stages place a premium on successfully developing an approach to stabilize all of the

components of the SRS assay with respect to storage, temperature and other environmental factors. These considerations include ease-of-use, sample size requirements, and the overall footprint of any new instrumentation. While important for use in a Biosafety Level 1 laboratory (BSL-1), these issues are markedly amplified if the target pathogen requires Biosafety Level 2 (BSL-2) or higher facilities. A BSL-1 laboratory can run tests on pathogens that pose minimal potential hazard to laboratory personnel and the environment, whereas more hazardous pathogens requires BSL-2 or and higher facilities. The higher infrastructure and operations cost of enhanced safety facilities amplify the importance of ease-of-use and a small instrument footprint. Again, the deployment trials in **Stage 7** will take advantage of partnerships with first adopters and other early-stage users to identify and provide feedback in order to fine tune procedures for ease-of-use platform architecture, and data archiving and analysis. Successfully passing through each of the stages will facilitate translation to end users and potential commercialization partners.

Summary and Prospectus

This paper has presented an overview of the status, opportunities, and obstacles faced as researchers begin to focus on the movement of SERS-based diagnostic tests for pathogens and other disease and health markers from the research and development laboratory to the clinical and POC arenas. At a fundamental level, innovations in nanostructured materials and plasmonics-based enhancement will continue to redefine the ability to detect markers by SERS at ever-lower levels, which, by extension, should improve clinical accuracy. It is now time, however, to focus on the

work needed to demonstrate the true potential of SERS as an exciting new addition to the diagnostics toolbox. This is a daunting task that is best addressed by forming integrative teams and partnerships with clinicians, biostatisticians, instrument and diagnostic kit manufacturers and other end users to deliver the promise and advance the realization of this goal. These include taking the steps: (1) to design and carry out a carefully organized series of validation studies using a set of well characterized “real world” specimens; (2) to improve ease-of-use; (3) to reduce the turn-around time from sample collection to actionable results; and (4) to construct an affordable, clinically accurate, and field deployable platform and a companion set of test kits. In fact, there are several efforts now underway that are attempting to execute this plan and we believe that the potential of SERS will begin to be realized in the next few years.

Acknowledgements

The authors gratefully acknowledge the many insightful and late night discussions with past and present members of our research group as well as suggestions from both reviewers. We are also highly appreciative of the support from the U.S. Food and Drug Administration’s Critical Paths Initiative, the National Cancer Institute’s Innovative Molecular Analysis Technologies (IMAT) Program, the National Institute of Allergy and Infectious Diseases Partnerships in Biodefense Program, the Bill and Melinda Gates Foundation, the Dengue Branch of the Centers for Disease Control, and the U.S. Army’s Dugway Proving Ground.

References

1. A. M. Caliendo, D. N. Gilbert, C. C. Ginocchio, K. E. Hanson, L. May, T. C. Quinn, F. C. Tenover, D. Alland, A. J. Blaschke, R. A. Bonomo, K. C. Carroll, M. J. Ferraro, L. R. Hirschhorn, W. P. Joseph, T. Karchmer, A. T. MacIntyre, L. B. Reller, A. F. Jackson and A. for the Infectious Diseases Society of, *Clin. Infect. Dis.*, 2013, **57**, S139-S170.
2. L. Garibyan and N. Avashia, *J. Invest. Dermatol.*, 2013, **133**, e6-e6.
3. R. M. Lequin, *Clin. Chem.*, 2005, **51**, 2415-2418.
4. L. Chang, D. M. Rissin, D. R. Fournier, T. Piech, P. P. Patel, D. H. Wilson and D. C. Duffy, *J. Immunol. Methods*, 2012, **378**, 102-115.
5. R. de la Rica and M. M. Stevens, *Nat Nano*, 2012, **7**, 821-824.
6. S. Heydari and G. H. Haghayegh, *J. Sens. Technol.*, 2014, **4**, 20.
7. S. Karmakar, S. Kumar, R. Rinaldi and G. Maruccio, *J. Phys.: Conf. Ser.*, 2011, **292**, 012002.
8. M. Pelton and G. W. Bryant, *Introduction to metal-nanoparticle plasmonics*, Wiley-Science Wise Co-Publication, Hoboken, NJ, 2013.
9. A. Barthélémy, A. Fert, J. P. Contour, M. Bowen, V. Cros, J. M. De Teresa, A. Hamzic, J. C. Faini, J. M. George, J. Grollier, F. Montaigne, F. Pailloux, F. Petroff and C. Vouille, *J. Magn. Magn. Mater.*, 2002, **242–245, Part 1**, 68-76.
10. G. A. Prinz, *Science*, 1998, **282**, 1660-1663.
11. J. A. Schuller, E. S. Barnard, W. Cai, Y. C. Jun, J. S. White and M. L. Brongersma, *Nat Mater*, 2010, **9**, 193-204.
12. N. J. Halas, *Nano Lett.*, 2010, **10**, 3816-3822.
13. H. A. Atwater, *Sci. Am.*, 2007, **296**, 56-62.
14. R. P. Van Duyne, *Science*, 2004, **306**, 985-986.
15. M. D. Sonntag, J. M. Klingsporn, A. B. Zrimsek, B. Sharma, L. K. Ruvuna and R. P. Van Duyne, *Chem. Soc. Rev.*, 2014, **43**, 1230-1247.
16. Y. B. Zheng, B. Kiraly, P. S. Weiss and T. J. Huang, *Nanomedicine*, 2012, **7**, 751-770.
17. A. G. Brolo, *Nat Photon*, 2012, **6**, 709-713.
18. E. Ringe, B. Sharma, A.-I. Henry, L. D. Marks and R. P. Van Duyne, *Phys Chem Chem Phys*, 2013, **15**, 4110-4129.
19. M. Moskovits, *Rev. Mod. Phys.*, 1985, **57**, 783-826.
20. P. L. Stiles, J. A. Dieringer, N. C. Shah and R. P. Van Duyne, *Annu. Rev. Anal. Chem.*, 2008, **1**, 601-626.
21. J. M. McMahon, S. Li, L. K. Ausman and G. C. Schatz, *J. Phys. Chem. C*, 2012, **116**, 1627-1637.
22. K.-i. Yoshida, T. Itoh, H. Tamaru, V. Biju, M. Ishikawa and Y. Ozaki, *Phys. Rev. B*, 2010, **81**, 115406.
23. K. C. Bantz, A. F. Meyer, N. J. Wittenberg, H. Im, O. Kurtulus, S. H. Lee, N. C. Lindquist, S.-H. Oh and C. L. Haynes, *Phys Chem Chem Phys*, 2011, **13**, 11551-11567.
24. M. M. Harper, K. S. McKeating and K. Faulds, *Phys Chem Chem Phys*, 2013, **15**, 5312-5328.
25. F. J. García-Vidal and J. B. Pendry, *Phys Rev Lett*, 1996, **77**, 1163-1166.
26. M. Fan, G. F. S. Andrade and A. G. Brolo, *Anal. Chim. Acta*, 2011, **693**, 7-25.
27. M. J. Mulvihill, X. Y. Ling, J. Henzie and P. Yang, *J. Am. Chem. Soc.*, 2010, **132**, 268-274.
28. T. M. Cotton, R. A. Uphaus and D. Mobius, *J. Phys. Chem.*, 1986, **90**, 6071-6073.
29. B. J. Kennedy, S. Spaeth, M. Dickey and K. T. Carron, *J. Phys. Chem. B*, 1999, **103**, 3640-3646.
30. K. Kneipp, Y. Wang, H. Kneipp, L. T. Perelman, I. Itzkan, R. R. Dasari and M. S. Feld, *Phys Rev Lett*, 1997, **78**, 1667-1670.

31. M. Fleischmann, P. J. Hendra and A. J. McQuillan, *Chem. Phys. Lett.*, 1974, **26**, 163-166.
32. M. G. Albrecht and J. A. Creighton, *J. Am. Chem. Soc.*, 1977, **99**, 5215-5217.
33. D. L. Jeanmaire and R. P. Van Duyne, *J. Electroanal. Chem.*, 1977, **84**, 1-20.
34. T. E. Rohr, T. Cotton, N. Fan and P. J. Tarcha, *Anal. Biochem.*, 1989, **182**, 388-398.
35. *United States Pat.,* 5,376,556, 1994.
36. H.-Y. Park, R. J. Lipert and M. D. Porter, Nanosensing: Materials and Devices, edited by M. Saif Islam, Achyut K. Dutta, Proceedings of SPIE Vol. 5593, pp. 464-477, 2004.
37. D. A. Stuart, A. J. Haes, C. R. Yonzon, E. M. Hicks and R. P. Van Duyne, *Nanobiotechnology, IEE Proceedings* -, 2005, **152**, 13-32.
38. F. Yan and T. Vo-Dinh, *Sens. Actuators, B*, 2007, **121**, 61-66.
39. M. D. Porter, R. J. Lipert, L. M. Siperko, G. Wang and R. Narayanan, *Chem. Soc. Rev.*, 2008, **37**, 1001-1011.
40. D. Graham and R. Goodacre, *Chem. Soc. Rev.*, 2008, **37**, 883-884.
41. K. Hering, D. Cialla, K. Ackermann, T. Dörfer, R. Möller, H. Schneidewind, R. Mattheis, W. Fritzsche, P. Rösch and J. Popp, *Anal. Bioanal. Chem.*, 2008, **390**, 113-124.
42. M. D. Porter, M. C. Granger, L. M. Siperko and R. J. Lipert, *ECS Trans.*, 2009, **16**, 3-22.
43. C. L. Zavaleta, B. R. Smith, I. Walton, W. Doering, G. Davis, B. Shojaei, M. J. Natan and S. S. Gambhir, *Proc. Natl. Acad. Sci.*, 2009, **106**, 13511-13516.
44. M. D. Porter, M. C. Granger, L. M. Siperko and R. J. Lipert, 2011.
45. L. Rodriguez-Lorenzo, L. Fabris and R. A. Alvarez-Puebla, *Anal. Chim. Acta*, 2012, **745**, 10-23.
46. S. McAughtrie, K. Faulds and D. Graham, *J. Photochem. Photobiol., C*, 2014, **21**, 40-53.
47. R. A. Tripp, R. A. Dluhy and Y. Zhao, *Nano Today*, 2008, **3**, 31-37.
48. Y. H. Ngo, W. L. Then, W. Shen and G. Garnier, *J. Colloid Interface Sci.*, 2013, **409**, 59-65.
49. T. Vo-Dinh, M. Y. K. Hiromoto, G. M. Begun and R. L. Moody, *Anal. Chem.*, 1984, **56**, 1667-1670.
50. B. Sharma, R. R. Frontiera, A.-I. Henry, E. Ringe and R. P. Van Duyne, *Mater. Today*, 2012, **15**, 16-25.
51. S. Uskoković-Marković, M. Jelikić-Stankov, I. Holclajtner-Antunović and P. Đurđević, *J. Med. Biochem.*, 2013, **32**, 96-103.
52. D. A. Henderson, *Science*, 1999, **283**, 1279-1282.
53. B. Graham, J. Talent, R. Larsen and L. Kidder, Bio-Response Report Card, http://www.biotech-now.org/health/2011/10/bioterrorism-ten-years-later.
54. J. Bordet and E. Renaux, *Ann. Inst. Pasteur (Paris)*, 1930, **45**, 1-25.
55. B. Moore and R. S. Williams, *Biochem. J.*, 1911, **5**, 181-187.
56. R. T. Hewlett and G. N. Hall, *J. Hyg.*, 1911, **11**, 473-480.
57. T. Vo-Dinh, G. D. Griffin and K. R. Ambrose, *Appl. Spectrosc.*, 1986, **40**, 696-700.
58. O. Lazcka, F. J. D. Campo and F. X. Muñoz, *Biosens. Bioelectron.*, 2007, **22**, 1205-1217.
59. S. K. Arya, A. Singh, R. Naidoo, P. Wu, M. T. McDermott and S. Evoy, *Analyst*, 2011, **136**, 486-492.
60. Y. H. Lai, S. Koo, S. H. Oh, E. A. Driskell and J. D. Driskell, *Anal. Methods*, 2015, **7**, 7249-7255.
61. A. H. Peruski, L. H. Johnson Iii and L. F. Peruski Jr, *J. Immunol. Methods*, 2002, **263**, 35-41.
62. M. Seaver, J. D. Eversole, J. J. Hardgrove, W. K. Cary and D. C. Roselle, *Aerosol Sci. Technol.*, 1999, **30**, 174-185.
63. N. Jouvenet, P. D. Bieniasz and S. M. Simon, *Nature*, 2008, **454**, 236-240.

64. H. Yu, J. W. Raymonda, T. M. McMahon and A. A. Campagnari, *Biosens. Bioelectron.*, 2000, **14**, 829-840.
65. R. Vidžiūnaité, N. Dikinienė, V. Miliukienė, P. Mikulskis and J. Kulys, *J. Biolumin. Chemilumin.*, 1995, **10**, 193-198.
66. L. A. Lane, X. Qian and S. Nie, *Chem. Rev.*, 2015, **115**, 10489-10529.
67. S. Nie and S. R. Emory, *Science*, 1997, **275**, 1102-1106.
68. D. S. Grubisha, R. J. Lipert, H.-Y. Park, J. Driskell and M. D. Porter, *Anal. Chem.*, 2003, **75**, 5936-5943.
69. X. Zhang, M. A. Young, O. Lyandres and R. P. Van Duyne, *J. Am. Chem. Soc.*, 2005, **127**, 4484-4489.
70. S. Xu, X. Ji, W. Xu, X. Li, L. Wang, Y. Bai, B. Zhao and Y. Ozaki, *Analyst*, 2004, **129**, 63-68.
71. J. D. Driskell, C. G. Larrick and C. Trunell, *Langmuir*, 2014, **30**, 6309-6313.
72. A. Lopez, F. Lovato, S. Hwan Oh, Y. H. Lai, S. Filbrun, E. A. Driskell and J. D. Driskell, *Talanta*, 2016, **146**, 388-393.
73. R. P. van Duyne, K. L. Haller and R. I. Altkorn, *Chem. Phys. Lett.*, 1986, **126**, 190-196.
74. K. L. Norrod, L. M. Sudnik, D. Rousell and K. L. Rowlen, *Appl. Spectrosc.*, 1997, **51**, 994-1001.
75. T. O. Deschaines and K. T. Carron, *Appl. Spectrosc.*, 1997, **51**, 1355-1359.
76. S. E. J. Bell and N. M. S. Sirimuthu, *Chem. Soc. Rev.*, 2008, **37**, 1012-1024.
77. L. Libioulle, Y. Houbion and J. M. Gilles, *Rev. Sci. Instrum.*, 1995, **66**, 97-100.
78. C. Burda, X. Chen, R. Narayanan and M. A. El-Sayed, *Chem. Rev.*, 2005, **105**, 1025-1102.
79. C. J. Murphy, T. K. Sau, A. M. Gole, C. J. Orendorff, J. Gao, L. Gou, S. E. Hunyadi and T. Li, *J. Phys. Chem. B*, 2005, **109**, 13857-13870.
80. W. E. Doering, M. E. Piotti, M. J. Natan and R. G. Freeman, *Adv. Mater.*, 2007, **19**, 3100-3108.
81. E. P. Hoppmann, W. W. Yu and I. M. White, *Appl. Spectrosc.*, 2014, **68**, 909-915.
82. P. M. Fierro-Mercado and S. P. Hernandez-Rivera, *Int. J. Spectrosc.*, 2012, **2012**, 7.
83. X. Zhou, W. Li, M. Wu, S. Tang and D. Liu, *Appl. Surf. Sci.*, 2014, **292**, 537-543.
84. X. Dou, T. Takama, Y. Yamaguchi, H. Yamamoto and Y. Ozaki, *Anal. Chem.*, 1997, **69**, 1492-1495.
85. S. P. Mulvaney, M. D. Musick, C. D. Keating and M. J. Natan, *Langmuir*, 2003, **19**, 4784-4790.
86. D. O. Ansari, D. A. Stuart and S. Nie, Proc. SPIE 5699, Imaging, Manipulation, and Analysis of Biomolecules and Cells: Fundamentals and Applications III, 82, doi:10.1117/12.591178, 2005.
87. J. D. Driskell, K. M. Kwarta, R. J. Lipert, M. D. Porter, J. D. Neill and J. F. Ridpath, *Anal. Chem.*, 2005, **77**, 6147-6154.
88. J. Ni, R. J. Lipert, G. B. Dawson and M. D. Porter, *Anal. Chem.*, 1999, **71**, 4903-4908.
89. H.-Y. Park, Iowa State University, 2005.
90. K. Faulds, W. E. Smith and D. Graham, *Analyst*, 2005, **130**, 1125-1131.
91. Y. C. Cao, R. Jin and C. A. Mirkin, *Science*, 2002, **297**, 1536-1540.
92. R. L. McCreery, M. Fleischmann and P. Hendra, *Anal. Chem.*, 1983, **55**, 146-148.
93. J. M. Bello, V. A. Narayanan, D. L. Stokes and T. Vo Dinh, *Anal. Chem.*, 1990, **62**, 2437-2441.
94. A. S. Fauci, *Clin. Infect. Dis.*, 2001, **32**, 675-685.
95. R. Lozano, et. al., *The Lancet*, 2012, **380**, 2095-2128.
96. NIH, National Institute of Allergy and Infectious Diseases (NIAID), NIAID Emerging Infectious Diseases/Pathogens, http://www.niaid.nih.gov/topics/BiodefenseRelated/Biodefense/Pages/CatA.aspx.

97. D. E. Gottschling, R. D. Grober and M. Sailor, in *Defense Science Study Group 1998-1999*, Institue for Defense Analyses, 2000, vol. Volume 1: Papers 1-13, pp. 187-206.
98. J. Christensen, L. Nørgaard, R. Bro and S. B. Engelsen, *Chem. Rev.*, 2006, **106**, 1979-1994.
99. L. He, E. Lamont, B. Veeregowda, S. Sreevatsan, C. L. Haynes, F. Diez-Gonzalez and T. P. Labuza, *Chem. Sci.*, 2011, **2**, 1579-1582.
100. G. A. Balint, *Toxicology*, 1974, **2**, 77-102.
101. R. Gao, J. Ko, K. Cha, J. Ho Jeon, G.-e. Rhie, J. Choi, A. J. deMello and J. Choo, *Biosens. Bioelectron.*, 2015, **72**, 230-236.
102. K. Ryu, A. J. Haes, H.-Y. Park, S. Nah, J. Kim, H. Chung, M.-Y. Yoon and S.-H. Han, *J. Raman Spectrosc.*, 2010, **41**, 121-124.
103. M. B. Wabuyele and T. Vo-Dinh, *Anal. Chem.*, 2005, **77**, 7810-7815.
104. H.-N. Wang, A. M. Fales, A. K. Zaas, C. W. Woods, T. Burke, G. S. Ginsburg and T. Vo-Dinh, *Anal. Chim. Acta*, 2013, **786**, 153-158.
105. H. T. Ngo, H.-N. Wang, A. M. Fales, B. P. Nicholson, C. W. Woods and T. Vo-Dinh, *Analyst*, 2014, **139**, 5655-5659.
106. S. Shanmukh, L. Jones, J. Driskell, Y. Zhao, R. Dluhy and R. A. Tripp, *Nano Lett.*, 2006, **6**, 2630-2636.
107. S. Shanmukh, L. Jones, Y. P. Zhao, J. D. Driskell, R. A. Tripp and R. A. Dluhy, *Anal. Bioanal. Chem.*, 2008, **390**, 1551-1555.
108. C. W. Burt and S. Schappert, National Center for Health Statistics, 2004, vol. 13.
109. K. Hadjigeorgiou, E. Kastanos, A. Kyriakides and C. Pitris, Proc. SPIE 8229, Optical Diagnostics and Sensing XII: Toward Point-of-Care Diagnostics; and Design and Performance Validation of Phantoms Used in Conjunction with Optical Measurement of Tissue IV, 82290D; doi:10.1117/12.907997., Cyprus, Greece, 2012.
110. E. K. Kastanos, A. Kyriakides, K. Hadjigeorgiou and C. Pitris, *J. Raman Spectrosc.*, 2010, **41**, 958-963.
111. H. Bottemiller, New Estimates Lower Incidence of Food Poisoning, http://www.foodsafetynews.com/2010/12/cdc-releases-new-foodborne-illness/#.VjEJeivv4o5.
112. H. Bottemiller, Annual Foodborne Illnesses Cost $77 Billion, Study Finds, http://www.foodsafetynews.com/2012/01/foodborne-illness-costs-77-billion-annually-study-finds/#.VjEMdyvv4o4.
113. M. N. Guerini, T. M. Arthur, S. D. Shackelford and M. Koohmaraie, *J. Food Prot.*, 2006, **69**, 1007-1011.
114. Y. Wang, S. Ravindranath and J. Irudayaraj, *Anal. Bioanal. Chem.*, 2011, **399**, 1271-1278.
115. J. Wang, X. Xie, J. Feng, J. C. Chen, X.-j. Du, J. Luo, X. Lu and S. Wang, *Int. J. Food Microbiol.*, 2015, **204**, 66-74.
116. E. J. Dufek, B. Ehlert, M. C. Granger, T. M. Sandrock, S. L. Legge, M. G. Herrmann, A. W. Meikle and M. D. Porter, *Analyst*, 2010, **135**, 2811-2817.
117. A. Assaf, C. B. Y. Cordella and G. Thouand, *Anal. Bioanal. Chem.*, 2014, **406**, 4899-4910.
118. K. L. Rule and P. J. Vikesland, *Environ. Sci. Technol.*, 2009, **43**, 1147-1152.
119. Associated-Press, Americans spent a record $56 billion on pets last year, http://www.cbsnews.com/news/americans-spent-a-record-56-billion-on-pets-last-year/.
120. C. o. V. M. Cornell University, ed. C. University, 2014, pp. 1-36.
121. B. J. Yakes, R. J. Lipert, J. P. Bannantine and M. D. Porter, *Clin. Vaccine Immunol.*, 2008, **15**, 227-234.
122. B. J. Yakes, R. J. Lipert, J. P. Bannantine and M. D. Porter, *Clin. Vaccine Immunol.*, 2008, **15**, 235-242.

123. K. Stevenson, *Cattle Practice*, 2012, **18**, 104-109.
124. V. J. Timms, M. M. Gehringer, H. M. Mitchell, G. Daskalopoulos and B. A. Neilan, *J. Microbiol. Methods*, 2011, **85**, 1-8.
125. K. Over, P. G. Crandall, C. A. O'Bryan and S. C. Ricke, *Crit. Rev. Microbiol.*, 2011, **37**, 141-156.
126. M. A. Firpo, K. M. Boucher and S. J. Mulvihill, *Theor Biol Med Model*, 2014, **11**, 34.
127. K. E. Poruk, M. A. Firpo, D. G. Adler and S. J. Mulvihill, *Ann. Surg.*, 2013, **257**, 17.
128. J. Ren, H. Cai, Y. Li, X. Zhang, Z. Liu, J.-S. Wang, Y. L. Hwa, Y. Zhang, Y. Yang, Y. Li and S.-W. Jiang, *Expert Rev. Mol. Diagn.*, 2010, **10**, 787-798.
129. A. A. Ellington, I. J. Kullo, K. R. Bailey and G. G. Klee, *Clin. Chem.*, 2010, **56**, 186-193.
130. J. A. Bastarache, T. Koyama, N. E. Wickersham, D. B. Mitchell, R. L. Mernaugh and L. B. Ware, *J. Immunol. Methods*, 2011, **367**, 33-39.
131. S. T. Chang, J. M. Zahn, J. Horecka, P. L. Kunz, J. M. Ford, G. A. Fisher, Q. T. Le, D. T. Chang, H. Ji and A. C. Koong, *J. Transl. Med.*, 2009, **7**, 105.
132. M. Pla-Roca, R. F. Leulmi, S. Tourekhanova, S. Bergeron, V. Laforte, E. Moreau, S. J. C. Gosline, N. Bertos, M. Hallett, M. Park and D. Juncker, *Mol. Cell. Proteomics*, 2012, **11**.
133. K. K. Maiti, U. S. Dinish, A. Samanta, M. Vendrell, K.-S. Soh, S.-J. Park, M. Olivo and Y.-T. Chang, *Nano Today*, 2012, **7**, 85-93.
134. G. Zheng, F. Patolsky, Y. Cui, W. U. Wang and C. M. Lieber, *Nat Biotech*, 2005, **23**, 1294-1301.
135. S. F. Kingsmore, *Nat. Rev. Drug Discovery*, 2006, **5**, 310-320.
136. D. Mabey, R. W. Peeling, A. Ustianowski and M. D. Perkins, *Nat Rev Micro*, 2004, **2**, 231-240.
137. J. F. Pierson-Perry, J. E. Vaks, A. P. Durham, C. Fischer, C. Gutenbrunner, D. Hillyard, M. V. Kondratovich, P. Ladwig and R. A. Middleberg, *EP17-A2 Evaluation of Detection Capability for Clinical Laboratory Measurement Procedures; Approved Guideline—Second Edition*, Clinical and Laboratory Standards Institute, 950 West Valley Road, Suite 2500, Wayne, PA 19087 USA, Second edn., 2012.
138. L. A. Currie, *Pure Appl. Chem.*, 1995, **67**, 1699.
139. D. C. Harris, *Quantitative Chemical Analysis*, W. H. Freeman and Company, New York, NY, 7th edn., 2007.
140. S. A. Glantz, *Primer of biostatistics*, 1997.
141. D. A. Armbruster and T. Pry, *Clin. Biochem. Rev.*, 2008, **29 Suppl 1**, S49-52.
142. J. Fan, S. Upadhye and A. Worster, *Can. J. Emerg. Med.*, 2006, **8**, 19-20.
143. K. Hajian-Tilaki, *Caspian J. Intern. Med.*, 2013, **4**, 627-635.
144. R. Ekins and P. Edwards, *Clin. Chem.*, 1997, **43**, 1824-1831.
145. J. H. Granger, M. C. Granger, M. A. Firpo, S. J. Mulvihill and M. D. Porter, *Analyst*, 2013, **138**, 410-416.
146. K. W. Kho, C. Y. Fu, U. S. Dinish and M. Olivo, *J. Biophotonics*, 2011, **4**, 667-684.
147. H. Chon, S. Lee, S.-Y. Yoon, S.-I. Chang, D. W. Lim and J. Choo, *Chem. Comm.*, 2011, **47**, 12515-12517.
148. X. Wang, X. Qian, J. J. Beitler, Z. G. Chen, F. R. Khuri, M. M. Lewis, H. J. C. Shin, S. Nie and D. M. Shin, *Canc. Res.*, 2011, **71**, 1526-1532.
149. R. Bro, *Anal. Chim. Acta*, 2003, **500**, 185-194.
150. P. K. Hopke, *Anal. Chim. Acta*, 2003, **500**, 365-377.
151. S. Wold, K. Esbensen and P. Geladi, *Chemom. Intell. Lab. Syst.*, 1987, **2**, 37-52.
152. K. Gracie, E. Correa, S. Mabbott, J. A. Dougan, D. Graham, R. Goodacre and K. Faulds, *Chem. Sci.*, 2014, **5**, 1030-1040.
153. R. Boqué and F. X. Rius, *Chemom. Intell. Lab. Syst.*, 1996, **32**, 11-23.

154. A. C. Olivieri, N. M. Faber, J. Ferré, R. Boqué, J. H. Kalivas and H. Mark, *Pure Appl. Chem.*, 2006, **78**, 633-661.
155. K. Faulds, R. Jarvis, W. E. Smith, D. Graham and R. Goodacre, *Analyst*, 2008, **133**, 1505-1512.
156. I. S. Patel, W. R. Premasiri, D. T. Moir and L. D. Ziegler, *J. Raman Spectrosc.*, 2008, **39**, 1660-1672.
157. R. Boqué, M. S. Larrechi and F. X. Rius, *Chemom. Intell. Lab. Syst.*, 1999, **45**, 397-408.
158. R. Boqué, N. M. Faber and F. X. Rius, *Anal. Chim. Acta*, 2000, **423**, 41-49.
159. P. Geladi, *Spectrochim. Acta, Part B*, 2003, **58**, 767-782.
160. S. Laing, K. Gracie and K. Faulds, *Chem. Soc. Rev.*, 2015, DOI: 10.1039/C5CS00644A.
161. P. Geladi, B. Sethson, J. Nyström, T. Lillhonga, T. Lestander and J. Burger, *Spectrochim. Acta, Part B*, 2004, **59**, 1347-1357.
162. K. C. Henderson, E. S. Sheppard, O. E. Rivera-Betancourt, J.-Y. Choi, R. A. Dluhy, K. A. Thurman, J. M. Winchell and D. C. Krause, *Analyst*, 2014, **139**, 6426-6434.
163. G. McNay, D. Eustace, W. E. Smith, K. Faulds and D. Graham, *Appl. Spectrosc.*, 2011, **65**, 825-837.
164. E. P. Diamandis and T. K. Christopoulos, *Immunoassay*, Academic Press, New York, NY, 1996.
165. D. Wild, *The Immunoassay Handbook*, Elsevier Ltd., Oxford, UK, Third edn., 2005.